Critical Elements of Electron-Bombardment Propulsion for Large Space Systems

D.C. Byers* and V.K. Rawlin†
NASA Lewis Research Center, Cleveland, Ohio

Presented are the results of an analysis of some critical elements of electron-bombardment ion propulsion systems for use in the transportation and on-orbit operations of large space systems. Using baseline technology from the ongoing primary propulsion program and other sources, preliminary estimates of the expected characteristics of key system elements such as thrusters and propellant storage systems have been performed. Projections of expected thruster performance on argon are presented based on identified constraints that limit the achievable thrust and/or power density of bombardment thrusters. Some system characteristics are then evaluated as a function of thruster diameter and specific impulse.

Nomenclature

d	= thruster diameter, cm
g	= acceleration due to gravity, 9.8 m/sec^2
J	= current, A
I_{sp}	= specific impulse, sec
M	= mass, kg
P	= thrust subsystem power, W
T	= thrust, N
$\overline{T}$	= maximum allowable grid temperature, K
Δt	= thrusting time, days
V	= accelerating voltage, V
ΔV	= mission velocity increment, m/sec
ϵ_I	= energy required per beam ion
η	= efficiency

Subscripts

B	= beam
F	= payload
N	= net
P	= propellant
T	= thrust subsystem
U	= propellant utilization

Introduction

THE application of electron-bombardment ion thruster subsystems has been analyzed in detail for a broad set of planetary[1-4] and near-Earth[5,6] missions. The thrust subsystems assumed for contemporary studies employed the 30-cm-diam mercury-bombardment ion thruster[7] presently under development. In general, these studies assumed shuttle-sized (or smaller) payloads.

Recently, studies have been performed on the characteristics and potentials of large space systems (LSS), which are significantly larger in final configuration than shuttle-sized payloads.[8-10] Examples of such systems are satellite power stations,[8,9] space manufacturing facilities,[10] and very large communication systems. Propellant requirements for these systems have been analyzed in some detail.[11,12] These studies have indicated that the propulsion system characteristics can impact the performance and cost of LSS very strongly. In particular, significant benefits are obtained by the use of high ($>$1500 sec) specific impulse propulsion for the orbit-to-orbit transportation function. For example, large cost savings accrue[11] from the use of high specific impulse propulsion because of the reduction in orbit transfer propellant which is required to be raised from Earth to low-Earth orbit (LEO). The on-orbit propulsion requirements also have been analyzed,[13] and the potential benefits of high specific impulse propulsion for on-orbit propulsion are analogous to those identified for the orbit transfer transportation function.

Several candidate propulsion concepts have been proposed for use with LSS. These include electron-bombardment thrusters,[7] magnetoplasmadynamic thrusters,[14] high specific impulse resistojets, and thermal rockets where the onboard propellant is heated by remotely based lasers.[15] Of these propulsion concepts, the electron-bombardment thruster is in the most advanced state of development and is capable of operation at the highest values of specific impulse.

The strong dependence of overall LSS performance and cost as a result of the propulsion subsystem characteristics was noted previously. Accurate projection of system benefits is difficult to assess unless the thrust subsystem characteristics are established.

This paper will discuss and evaluate some of the critical elements and performance characteristics of electron-bombardment subsystems which are pertinent to the design of LSS. A brief review of LSS propulsion requirements will be presented to aid the selection of key concept options. A discussion follows on the selection and storage requirements of thruster propellant. Analysis of the expected performance and characteristics of bombardment thrusters then is presented, followed by a brief discussion of power processing requirements for the proposed thrust subsystem approaches.

LSS Propulsion Requirements

The selection of thrust subsystem design and operating characteristics will ultimately depend, of course, on the ability of a particular propulsion subsystem to satisfy the overall system requirements. These requirements will include the usual propulsion performance parameters such as specific impulse, thrust, lifetime, and system dry mass and volume. In addition, many other characteristics such as potential ecological impact, availability of materials, refurbishment capability, and propulsion system cost will likely be of extreme concern for the scale of propulsion subsystems required for LSS.

The propulsion subsystem requirements will be sensitive to system approach options.[11,12] These options include the degree of LEO assembly assumed, constraints on transportation trip time, launch and orbit transfer strategy, orbit transfer and on-orbit payload design, power source assumptions, and on-orbit design lifetime. Detailed consideration of

Presented as Paper 76-1039 at the AIAA International 12th Electric Propulsion Conference, Key Biscayne, Fla., Nov. 15-17, 1976; submitted Jan. 28, 1977; revision received July 22, 1977.

Index categories: Electric and Advanced Space Propulsion; Spacecraft Propulsion Systems Integration; Engine Performance.

*Head, Electric Thruster Section. Member AIAA.

†Aerospace Engineer.

such options is beyond the scope of this paper. Some calculations defining the propellant, thrust, and power required for the transportation of large space system were presented in Ref. 16. As examples, Figs. 1 and 2 present the required thrust and power, respectively, as a function of the ratio of payload mass to trip time with specific impulse as a parameter. The mission parameters assumed for the data of Figs. 1 and 2 were 1) orbit transfer from 352 km to geosynchronous altitude, 2) a 28.5 deg plane change, and 3) a total velocity increment of 5770 m/sec. For the purposes of this paper, many secondary factors such as occultation, attitude-control requirements during transfer, and penalties associated with low vs high thrust were ignored.

Figure 1 shows that the required thrust is most strongly a function of the ratio of payload mass to trip time, and becomes relatively insensitive to specific impulse above about 2000 sec. As seen in Fig. 2, the required power, at fixed thrust subsystem efficiency, increases slightly less than linearly with increasing specific impulse. This behavior reflects the decrease in thrust required as specific impulse increases.

On-orbit propulsion requirements[13] also were reviewed in Ref. 16 and compared with transportation propulsion requirements for a 11.4×10^6-kg satellite. The on-orbit thrust levels were found to be more than an order of magnitude less than those during the transportation phase for transfer times less than 1000 days. However, as seen in Fig. 3, for LSS lifetimes of interest[11] (up to 30 yr), the on-orbit total impulse can be of the same order as that required for the transportation function. Selection of propulsion subsystems clearly must consider both the on-orbit and transportation functions, and it is likely that thrust subsystems with somewhat different characteristics will be optimal for these two functions.

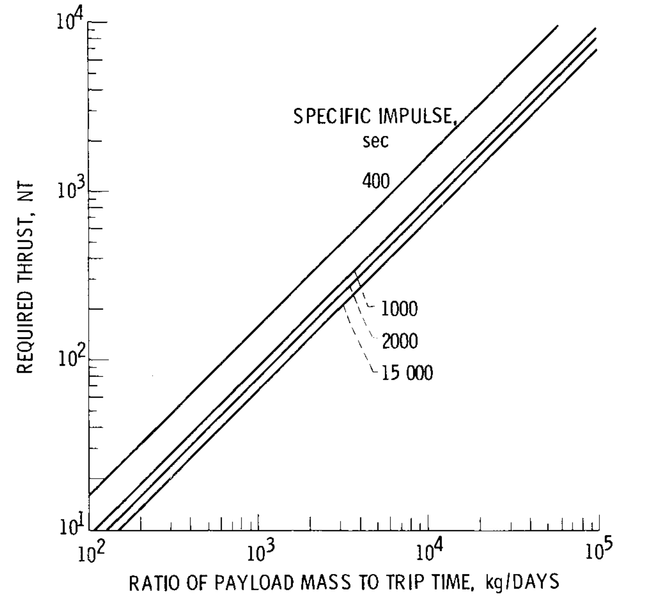

Fig. 1 Required thrust as a function of the ratio of payload mass to trip time. Orbit transfer from 352 km to geosynchronous altitude with 28.5-deg plane change.

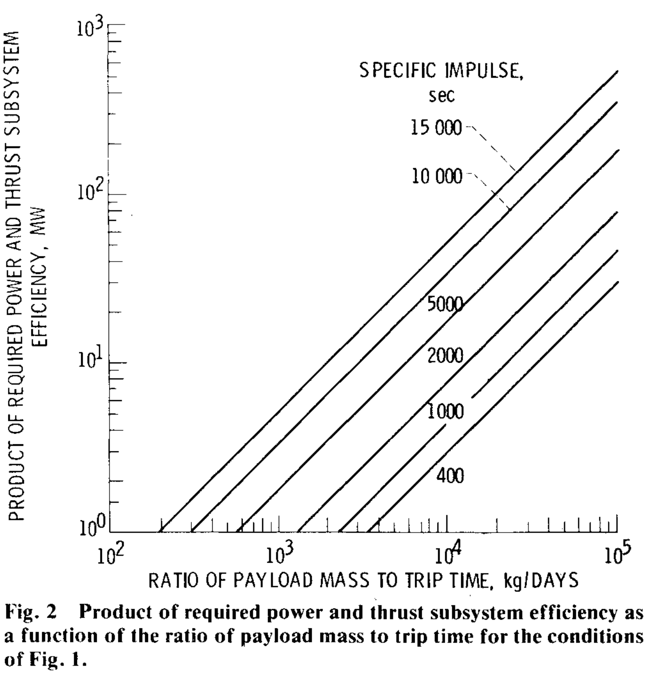

Fig. 2 Product of required power and thrust subsystem efficiency as a function of the ratio of payload mass to trip time for the conditions of Fig. 1.

Propellant Selection and Storage

Propellant Selection

Bombardment thrusters have been operated successfully over a wide range of conditions with a large variety of propellants.[17] Elemental propellants ranging in mass from hydrogen to mercury have been tested, along with some heavy molecules. Thruster performance as a function of propellant has been discussed and theoretical considerations presented by many authors,[18,19] with a review by Kaufman[18] being one of the most general and recent.

Based on the magnitude of propellant requirements for LSS, it is the opinion of the authors that propellant selection will be driven by the constraints of propellant availability, ecological impact, and cost. As pointed out in Ref. 16, argon and xenon appear to be the most promising candidate propellants, and argon was selected for detailed analysis on the basis of availability and cost. For comparison, the thrust-to-power ratio and specific impulse for xenon would vary nearly directly and inversely, respectively, as the square root of the ratio of the atomic masses of xenon and argon.

Propellant Storage

To fully describe the impact of selection of a particular propellant, it is necessary to evaluate the storage penalties associated with that propellant. A brief review of pertinent

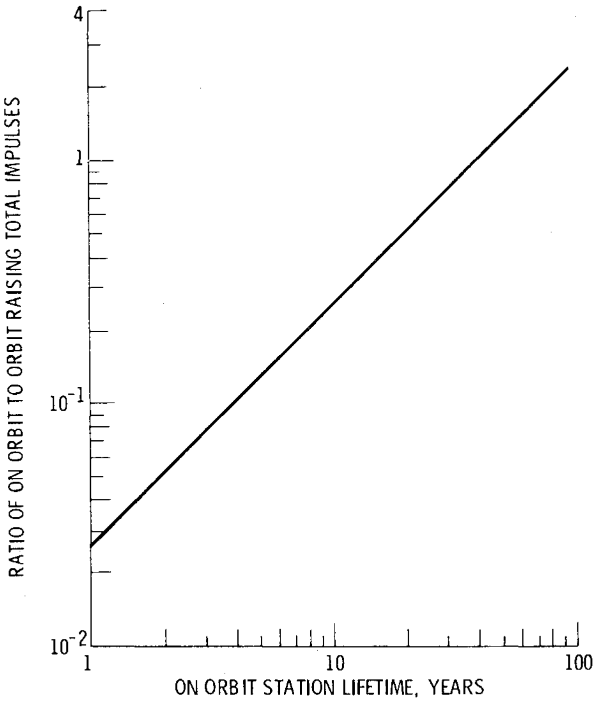

Fig. 3 Ratio of the total impulses for on-orbit and orbit-raising propulsion as a function of an on-orbit station lifetime (payload mass, 11.4×10^6 mg; specific impulse, 13,000 sec).

data was made with the object of providing a rough estimate of storage requirements with argon propellant to determine if the tankage was a significant mass relative to the propellant. Propellant storage has been the subject of intense development for many years.[20] Concepts for storage of liquid hydrogen and liquid oxygen have been systematically studied and developed for chemical rocket systems. The thermodynamic vent/screen baffle cryogenic storage system (hereinafter called TCSS) is one such concept.[21] This concept includes a vacuum jacket, and outflow of propellant is used for cooling purposes.

A preliminary analysis was performed to estimate the tankage mass with argon propellant.[22] A tank capable of holding 20,000 kg of liquid argon at 1.4×10^5 N/m^2 (20 psia) was assumed, and a mass breakdown is given in Table 1. A steady argon output flow of 5×10^{-5} kg/sec for the purpose of cooling was assumed and was found adequate to balance all expected thermal inputs to the propellant tank. The required propellant flow rate for cooling purposes will vary with tank size. The very large ratio of propellant mass to required coolant rate of propellant (about 0.4×10^9 sec for the design point) indicates that the TCSS concept could be used with negligible propellant loss without the requirement of active cooling systems.

Figure 4 shows the tankage mass fraction obtained by extrapolation of the single point design of Ref. 22. This extrapolation was made by assuming that the ratio of the masses of propellant to tankage scaled directly as the diameter of the tank. As seen in Fig. 4, tankage mass fraction less than 4.0% can be obtained for propellant loads greater than 20,000 kg. The mass of the propellant tankage is, therefore, not likely to be a driver in the mass of an electron-bombardment propulsion system.

Thruster Performance and Characteristics

General Description

The 30-cm-diam engineering model thruster (EMT) has been developed for use with mercury propellant. Detailed descriptions of the design and operation of this thruster have been given elsewhere, and the following discussion will be directed at describing the expected characteristics of argon-bombardment thrusters.

The performance of several different-size bombardment thrusters operated with argon has been reported in Refs. 17 and 23-25. In general, operation of the thruster with argon was similar to that with mercury. The discharge chamber losses, expressed as energy per beam ion (ϵ_I), were similar for both propellants, but the propellant utilization efficiency (η_u) was always lower with argon. When investigated, the ion extraction capability of the grid system varied with the mass of the ion used as expected.

Many features of the thruster, such as the structure, insulators, and cabling, are passive and would not impact the performance of a thruster operated on argon. Those features that would be expected to constrain thruster performance or require modifications for operation with argon will be discussed below.

Ion Acceleration System

Recently, Sovey[25] has experimentally determined a relationship that predicts the maximum ion current density (for argon, xenon, and mercury) for grid systems that are near the minimum spacing expected to be attainable for large dished grid systems. Assuming operation at a maximum ratio of net-to-total ion accelerating voltage of 0.9 and a screen grid open area fraction of 0.7, Sovey's relationship for argon propellant may be expressed as

$$J_B/d^2 = 0.63 \times 10^{-9} V_N^{\,2.25} \tag{1}$$

In Eq. (1), it is seen that the beam current density rises very strongly with increasing net accelerating voltage. Earlier discussions stressed the desire to operate at high values of specific impulse (I_{sp}), which is proportional to the square root of V_N. But V_N cannot be increased without limit because there is, for any given grid spacing, a maximum total accelerating voltage that may be applied to the grids without continuous high-voltage breakdowns. Although the maximum allowable V_N increases as the grid spacing is increased, the beam current density of Eq. (1) decreases because it is inversely proportional to approximately the square of the grid spacing. In addition, the maximum allowable field strength decreases as the grid spacing is increased at a rate such that maximum value of beam current density occurs at the minimum possible grid spacing. For the near-minimum spacing of 0.6 mm, the value used for Eq. (1), the maximum value of V_N was assumed to be 5000 V, which corresponds to an I_{sp} of about 13,000 sec at a propellant utilization efficiency (η_u) of 0.82.

Discharge Power

The major power loss of the thruster occurs in the discharge chamber, where a large fraction of the discharge power is lost to the discharge chamber walls. Heating of passive thruster components, cathodes and grids excluded, can limit thruster operation only if component temperatures reach the limits of structural or chemical integrity. It has been shown by Sovey[25] that cathodes can be designed to operate at temperatures commensurate with long lifetimes at elevated emission current levels required by thrusters operated at high beam currents. In addition, when necessary, multiple cathodes may be used for larger thrusters.

The only active component expected to limit thruster performance as a result of elevated discharge power levels is the ion acceleration system. Tests of mercury-bombardment thrusters with diameters up to 150 cm have been conducted[26] in which the ion acceleration grid temperatures and discharge powers used were noted. As discussed in Ref. 16, analysis of these data leads to the following expression for the maximum beam current density:

$$J_B/d^2 = 2.507 \times 10^{14} (\overline{T})^4 \tag{2}$$

Table 1 Component masses for 20,000-kg argon thermodynamic cryogenic storage system[22]

Component	Mass, kg
Girth ring	141
Tank	45
Shield	69
Multilayer insulation	48
Vacuum jacket	340
Internal support	5
Contingency	90
Subtotal	738
Propellant	20,000
Total	20,738

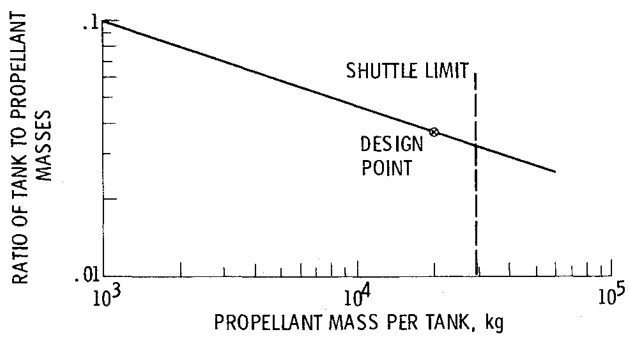

Fig. 4 Ratio of tank to propellant masses as a function of the propellant mass per tank.

Thus, for a selected average grid temperature, the beam current density limit is constant. Because the grids are made of molybdenum, there does not appear to be a materials problem at expected temperatures. Reference values of creep[27,28] indicate negligible dimensional changes even at temperatures of 1900 K over several hundreds of thousands of hours.

Dished grids were designed to move in a predetermined axial direction when they were subjected to changes in temperature. Use of the equations presented in Ref. 29 indicates that the reductions in grid-to-grid spacings resulting from hotter grid temperatures can be eliminated easily by increasing the dish depth during fabrication. In addition, there are no requirements for radiators to cool the thruster components. For this study, $\bar{T}$ was chosen arbitrarily to be 913 K (700°C), less than a factor of 2 greater than the temperatures of the present EMT.

Thruster Performance

Figure 5 shows the three ion accelerating system operating limitations for a grid spacing of 0.6 mm. The "perveance" limit [Eq. (1)] determines the minimum value of V_N required to obtain a given beam current density. At a value of V_N of 2774 V, or I_{sp}/η_u of about 11,000 sec, the selected maximum average grid temperature limit of 700°C limits the ratio of beam current to square of thruster diameter to 0.0225 A/cm^2. The maximum allowable field strength limit specifies practical maximum values of V_N of 5000 V or I_{sp}/η_u of nearly 16,000 sec. This maximum in specific impulse is a result of the assumption of close-spaced ion accelerator grids. This assumption was adopted because the maximum thrust density (and, hence, the minimum number of thrusters for a particular thrust level) is achieved with close-spaced accelerator grids. Specific impulse in excess of 16,000 sec can be obtained with thrusters that use large-spaced grids, and values up to 25,000 sec have been demonstrated with mercury propellant[30] (equivalent to about 55,000 sec with argon). Use of large-spaced grids does, however, strongly limit the thrust density and for that reason was not considered herein.

Using the beam current density limitations of Fig. 5, the thrust and power density limitations were calculated and are shown in Fig. 6 as a function of the ratio of specific impulse to propellant utilization efficiency. For values of I_{sp}/η_u less than 11,000 sec, both parameters decrease rapidly as the I_{sp}/η_u is decreased. As the value of I_{sp}/η_u is increased from 11,000 to 16,000 sec, the thrust and power densities continue to increase but at a slower rate.

As the power to the thruster increases, the discharge and fixed power losses become nearly negligible when compared to the beam power, so that the total thruster efficiency approaches the propellant utilization efficiency. This is shown in Fig. 7, where the total efficiency is plotted as a function of

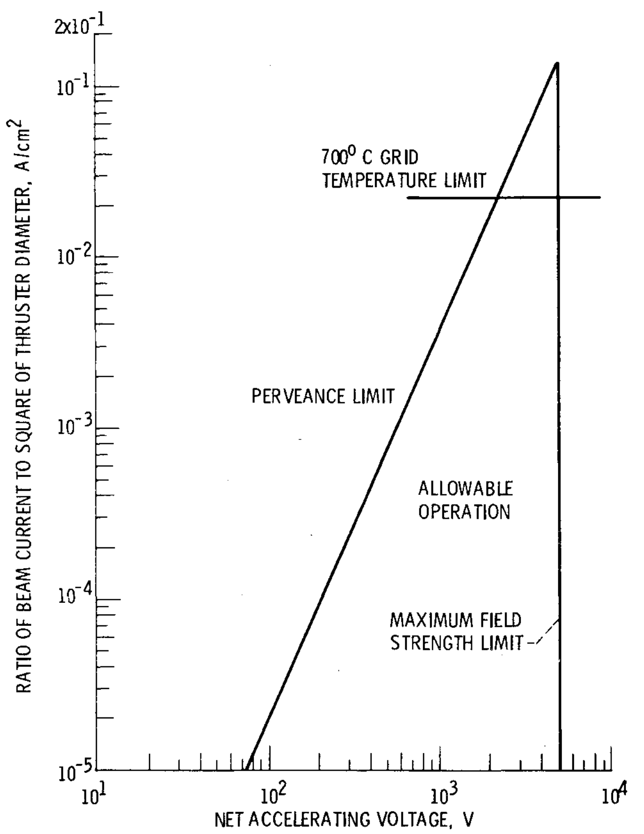

Fig. 5 Ratio of beam current to the square of thruster diameter as a function of the net accelerating voltage.

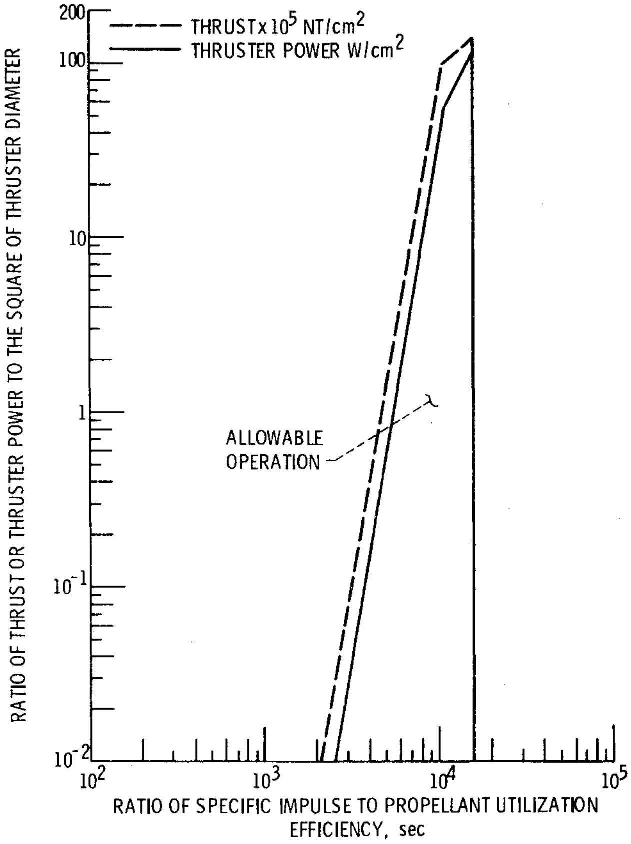

Fig. 6 Ratio of thrust or thruster power to the square of thruster diameter as a function of the ratio of specific impulse to propellant utilization efficiency.

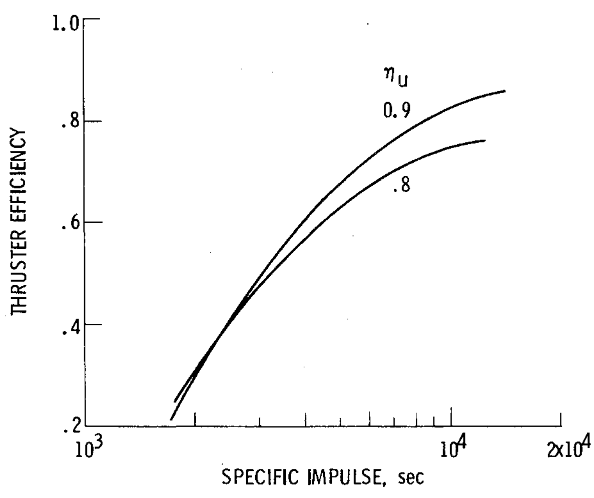

Fig. 7 Argon thruster efficiency as a function of specific impulse.

specific impulse. The thruster performance presented in this section has not been corrected for expected thrust losses such as beam divergence and multiply charged ions. It is expected that those corrections would result in decreases in thruster efficiency from about 5 to 10%.

Figure 8 shows the expected thrust and power per thruster as a function of thruster diameter. Also, Fig. 9 shows the number of various-size thrusters required to perform orbit transfer functions as a function of the ratio of payload mass to trip time. The number of 100-cm argon thrusters required for a particular mission is about 1130 times less than the required number of standard 30-cm mercury thrusters.

Thruster Scaling

Bombardment thrusters with diameters of 2.5, 5, 8, 10, 15, 20, 30, 50, and 150 cm have been tested. Whenever the size of the thruster was varied, the performance obtained at that particular time was nearly as expected based on developed scaling laws. The improvements in thruster performance which have occurred over the years have been applied successfully to thrusters of different size than those for which the improvement first occurred.

Most bombardment thrusters are cylindrical in shape, and therefore their volume may be defined by a length and a diameter. In addition, Kaufman[18] has noted that optimized thruster length changes little as the diameter is varied. Thus, to scale the operating or performance parameters of various-size thrusters, only the diameter need be varied.

Presently, 8[31] and 30[7] cm diam thrusters are at an advanced stage of development. Since this represents nearly a four-to-one increase in thruster diameter with less than a 50% increase in thruster length, it is expected that the thruster diameter may be increased to 100 cm with minor performance variations. The major modifications would be expected to occur with cathodes and ion extraction systems. Thrusters larger than 50 cm diam would probably use multiple cathodes for improved lifetime, reliability, and performance. The use of dished grids to maintain a close spacing over a 30 cm diam has proven to be quite successful. Presently, there do not appear to be any technological reasons to prohibit the fabrication of dished grids with diamters up to 100 cm diam (although materials such as molybdenum do not appear to be available presently in such sizes).

Thruster Mass

The mass per thruster as a function of thruster diameter was estimated by applying the following assumptions. For large space systems, the use of a shuttle launch vehicle and new packaging techniques were assumed which permitted substantial reductions in the masses of structural components.

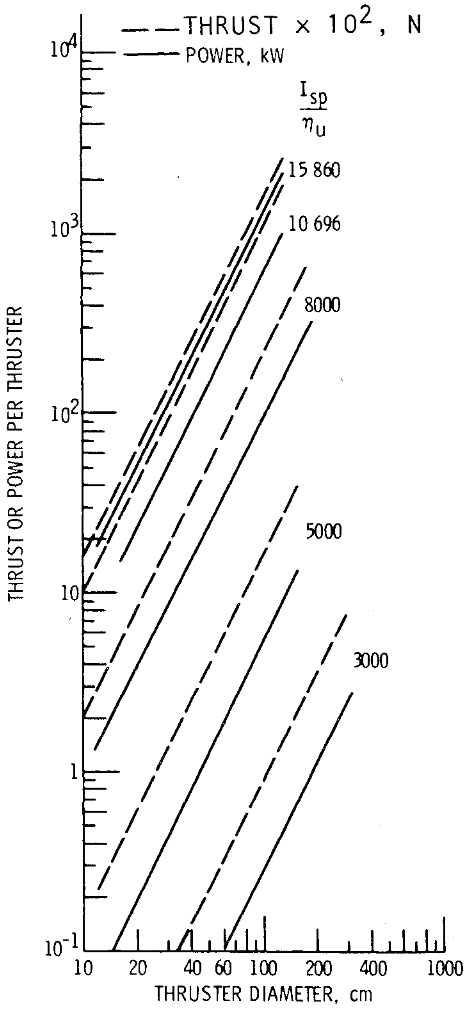

Fig. 8 Thrust or power per thruster as a function of thruster diameter (argon propellant).

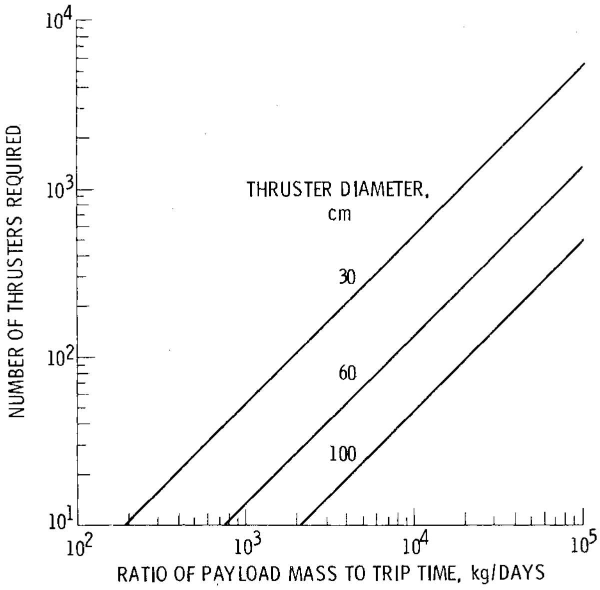

Fig. 9 Number of argon thrusters required as a function of the ratio of payload mass to trip time for the conditions of Fig. 1 (specific impulse, 13,000 sec; propellant utilization efficiency, 0.82).

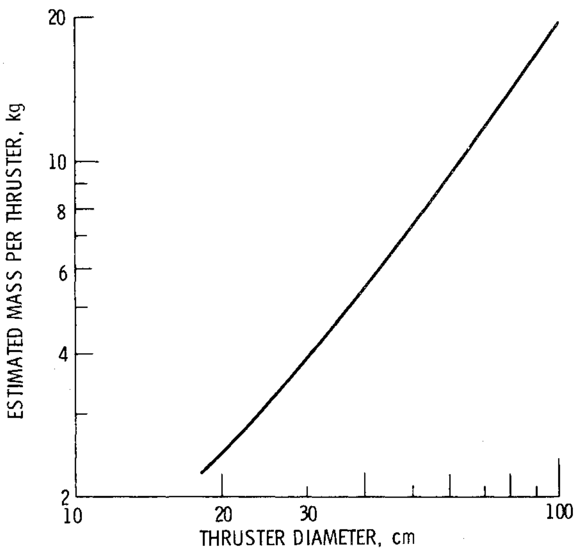

Fig. 10 Estimated mass of argon thrusters as a function of thruster diameter.

Table 2 Thruster input power summary

Parameter	30-cm mercury thruster	60-cm argon thruster	
Specific impulse, sec	2840	8770	13,000
Beam power, kW	2.2	184.2	405.0
Discharge power, kW	0.4	16.2	16.2
Fixed power, kW	0.05	0.1	0.1
Total power, kW	2.65	200.5	421.3

Mass reductions were also assumed when the high-voltage propellant isolators required with mercury propellant were redesigned for use with argon. With the use of these assumptions, the mass of a 30-cm-diam thruster was reduced from 8.2 kg (mercury EMT) to about 3.8 kg. The thruster components were then separated into four groups with masses that were either fixed, varied with thruster diameter or the square of diameter, or varied in discrete increments as the thruster size increased, such as multiple cathodes. The thruster diameter was then varied, and component masses were computed to obtain Fig. 10, which gives the estimated thruster mass as a function of thruster diameter.

Power Conditioning

The thruster power conditioning requirements and characteristics are influenced strongly by the mission and the power source selected and therefore will be discussed only briefly. The input power to the thruster consists of three major elements: the beam (ion acceleration) power, the discharge (propellant ionization) power, and a small amount of additional (other) power used to control the thruster which experience has shown is relatively insensitive to thruster size. The relative magnitudes of these powers are shown in Table 2 for the baseline 30-cm engineering model thruster (EMT) with mercury propellant and also for a 60-cm argon thruster at two values of specific impulse. As shown in Table 2, the beam power is the major power demand of a thruster, with the discharge power next. The other, nearly fixed, losses represent a negligible fraction of the thruster power, especially at high specific impulse.

All thruster input power is conditioned with the baseline 30-cm EMT system.[32] The resultant power conditioning specific mass, including thermal control for the power conditioner, is about 13 kg/kW for each 3-kW thruster system. Some estimates have been presented in Ref. 33 of the characteristics of electric propulsion power conditioning to be expected in the the future for large (up to 1000 kW) systems. Reference 33 indicated that reductions in specific mass ranging from about a factor of 3 to a factor of 10 might be expected in the time scale between the years 1985 and 2000.

Another approach has been demonstrated which could reduce the power conditioning requirements more drastically. For the approach, the ion beam power was obtained directly from a solar array on 8-[34], 15-[35], and 30-[36] cm electron-bombardment mercury thrusters. The discharge was also operated directly from an array for 15-[35] and 30-[36] cm thrusters. The operation of the beam and discharge from an array was accomplished in a straight-forward fashion in all cases, and the characteristics of the solar array output (such as low-ripple and inherent current-limited output) were well matched to the thruster requirements. When applied to a 60-cm argon thruster, direct operation from a solar array would require conditioning of only about 100 W of power (Table 2), thereby reducing the specific mass of the thrust subsystem.

Concluding Remarks

LSS propulsion requirements are far beyond those for which the present electron-bombardment thruster systems are being developed. A review of those requirements indicated that a propellant other than mercury should be selected. Argon was selected, based on availability, potential environmental impact, and present costs. Estimates of propellant storage requirements for argon were reviewed and found to be a small fraction of the propellant mass.

The performance characteristics of electron-bombardment thrusters operated on argon were reviewed and limitations discussed. The maximum values of output thrust were found to be very sensitive to the specific impulse selected and limited by the perveance, temperature, or breakdown characteristics of the ion accelerating system. Projection of the expected thruster performance and mass as a function of thruster diameter was presented. Finally, a brief review of present and potential advanced power conditioning was presented.

References

[1] Atkins, K.L., "Mission Applications of Electric Propulsion," AIAA Paper 74-1085, San Diego, Calif., 1974.

[2] Duxbury, J.H. and Finke, R.C., "A Candidate Mission Using the Shuttle and Solar Electric Propulsion," American Astronautical Society, Paper 75-163, Denver, Colo., 1975.

[3] Guttman, G.G., Gilbert, J., Horio, S.P., and Richardson, E.H., "The Solar Electric Propulsion Stage Concept for High Energy Missions," AIAA Paper 72-465, Bethesda, Md., 1972.

[4] Sauer, C., "Trajactory Analysis and Performance for SEP Comet Encke Missions," AIAA Paper 73-1059, Lake Tahoe, Nev., 1973.

[5] "Payload Utilization of SEPS," Boeing Aerospace Co., Seattle, Wash., D-180-19783-1, July 1976.

[6] "Extended Definition Feasibility Study for a Solar Electric Propulsion Stage, Volume 2," North American Rockwell, Downey, Calif., SD72-SA-0177-2-1, Jan. 1973.

[7] Schnelker, D.E. and Collett, C.R., "30-Cm Engineering Model Thruster Design and Qualification Tests," AIAA Paper 75-341, New Orleans, La., 1975.

[8] Glaser, P.E., "Evolution of the Satellite Solar Power Station SSPS Concept," *Journal of Spacecraft and Rockets,* Vol. 13, Sept. 1976, pp. 573-576.

[9] Grey, J., "The Outlook for Space Power," *Astronautics & Aeronautics,* Vol. 14, Oct. 1976, pp. 29-36.

[10] O'Neill, G.K., "Engineering a Space Manufacturing Center," *Astronautics & Aeronautics,* Vol. 14, Oct. 1976, pp. 20-28.

[11] "Initial Technical, Environmental, and Economic Evaluation of Space Solar Power Concepts. Volume 2: Detailed Report," Lyndon B. Johnson Space Center, Houston, Texas, JSC-11568-Vol. 2, Aug. 1976; also NASA TM X-74310, 1976.

[12] Stearns, J.W., "Large-Payload Earth-Orbit Transportation with Electric Propulsion," Jet Propulsion Lab., Pasadena, Calif., JPL-TM-33-793, Sept. 1976.

[13] Nathan, A., "Space-Based Solar Power Conversion and Delivery Systems (Study)," Grumman Aerospace Corp., Bethpage, N.Y., NSS-P-76-006, Oct. 1975.

[14] Esker, D.W., Kroutil, J.C., and Checkley, R.J., "Radiation Cooled MPD Arc Thruster," McDonnell-Douglas Corp., St. Louis, Mo., MDC-H296, July 1969; also NASA CR-72557, 1969.

[15] Moeckel, W.E., "Optimum Exhaust Velocity for Laser-Driven Rockets," *Journal of Spacecraft and Rockets,* Vol. 12, Nov. 1976, pp. 700-701.

[16] Byers, D.C. and Rawlin, V.K., "Electron Bombardment Propulsion System Characteristics for Large Space Systems," AIAA Paper 76-1039, Key Biscayne, Fla., 1976.

[17] Byers, D.C. and Reader, P.D., "Operation of an Electron-Bombardment Ion Source Using Various Gases," NASA TN D-6620, 1971.

[18] Kaufman, H.R., "Technology of Electron-Bombardment Ion Thrusters," *Advances in Electronics and Electron Physics,* Vol. 36, Academic Press, New York, 1974, pp. 265-373.

[19] Milder, N.L., "A Survey and Evaluation of Research on the Discharge Chamber Plasma of Kaufman Thruster," *Journal of Spacecraft and Rockets,* Vol. 7, June 1970, pp. 641-649.

[20] Stark, J.A., Blatt, M.H., Bennett, F.O., and Campbell, B.J., "Fluid Management Systems Technology Summaries," General Dynamics/Convair, San Diego, Calif., CASD-NAS-74-068, Dec. 1974; also NASA CR-134748, 1974.

[21] Cady, E.C., "Design and Evaluation of Thermodynamic Vent/Screen Baffle Cryogenic Storage System for Space Shuttles, Space Tugs, and Spacelab," McDonnell Douglas Astronautics Co., Huntington Beach, Calif., MDC-G5979, June 1975; also NASA CR-134810, 1975.

[22]Cady, E.C., private communication, McDonnell Douglas Astronautics Co., Huntington Beach, Calif., 1975.

[23]Reader, P.D., "The Operation of an Electric Bombardment Ion Source with Various Gases," *First International Conference on Electron and Ion Beam Science and Technology,* edited by R. Bakish, Wiley, New York, 1965, pp. 925-935.

[24]Schertler, R.J., "Preliminary Results of the Operation of a SERT II Thruster on Argon," AIAA Paper 71-157, New York, 1971.

[25]Sovey, J.S., "A 30-cm Diameter Argon Ion Source," AIAA Paper 76-1017, Key Biscayne, Fla., 1976.

[26]Nakanishi, S. and Pawlik, E.V., "Experimental Investigation of a 1.5-M-Diameter Kaufman Thruster," AIAA Paper 67-725, Colorado Springs, Colo., 1967.

[27]Green, W.V., Smith, M.C., and Olson, D.M., "Short-Time Creep-Rupture Behavior of Molybednum at High Temperatures," *Transactions of the Metallurgical Society of AIME,* Vol. 215, Dec. 1959, pp. 1061-1066.

[28]Carvalhinhos, H. and Argent, B.B., "The Creep of Molybdenum," *Journal of the Institute of Metals,* Vol. 95, 1967, pp. 364-368.

[29]Rawlin, V.K., Banks, B.A., and Byers, D.C., "Design, Fabrication, and Operation of Dished Accelerator Grids on a 30-cm Ion Thruster," AIAA Paper 72-486, Bethesda, Md., 1972.

[30]Byers, D.C., "An Experimental Investigation of a High-Voltage Electron-Bombardment Ion Thruster," *Journal of the Electrochemical Society,* Vol. 116, Jan. 1969, pp. 9-17.

[31]Banks, B.A. et al., "8-cm Mercury Ion Thruster System Technology," AIAA Paper 74-1116, San Diego, Calif., 1974.

[32]Cake, J.E., Sharp, G.R., Oglebay, J.C., Shaker, F.J., and Zavesky, R.J., "Modular Thruster Subsystem Approaches to Solar Electric Propulsion Module Design," AIAA Paper 76-1062, Key Biscayne, Fla., 1976.

[33]"A Forecast of Space Technology, 1980-2000," NASA SP-387, 1976.

[34]Stover, J.B., "System Tests with Electric Thruster Beam and Accelerator Directly Powered from Laboratory Solar Arrays," NASA TM X-3353, 1976.

[35]Sater, B.L., "The Advantages of the High Voltage Solar Array for Electric Propulsion," AIAA Paper 73-1103, Lake Tahoe, Nev., 1973.

[36]Gooder, S., private communication, NASA Lewis Research Center, Cleveland, Ohio, 1976.